






Experimental Study of Modified Absorber Plate Integrated with Aluminium Foam of Solar Water Heating System

Muhammad Hasan Basri^{*,***} , Jalaluddin ^{**†} , Rustan Tarakka ^{***} , Muhammad Syahid ^{***} ,
M. Anis Ilahi Ramadhani ^{*} 

* Graduate Student in Mechanical Engineering Department, Hasanuddin University, Gowa, 92171, Indonesia

** Department of Mechanical Engineering, Hasanuddin University, Gowa, 92171, Indonesia

*** Department of Mechanical Engineering, Tadulako University, Palu, 94118, Indonesia

(muhasanbasri77@gmail.com, jalaluddin_had@yahoo.com, rustan_tarakka@yahoo.com, syahid.arsjad@gmail.com, muhammad.anis09@gmail.com)

† Corresponding Author; Jalaluddin, Department of Mechanical Engineering, Hasanuddin University, Gowa, 92171, Indonesia,
Tel: +62411 586015, Fax: +62411 586015, jalaluddin_had@yahoo.com

Received: 04.04.2022 Accepted: 06.05.2022

Abstract- The Solar Water Heating System (SWHS) is a water heater equipment that utilizes solar energy for domestic scale needs. The potential generated by this system can reduce the energy demand of the building sector, reduce peak demand for electricity, and reduction in pollution. This study aims to analyze the performance of SWHS experimentally by modifying the addition of aluminium foam material at the bottom of the absorber plate and the top of the absorber plate. The absorber plate models are Standard Flat-Plate (SFP), SFP with Bottom Aluminium Foam (SFP-BAF), and SFP with Top Aluminium Foam (SFP-TAF). The experimental study was carried out for the three models under similar conditions using a Solar Thermal Energy Unit. The effect of flowrate variations and slope angles were also investigated. The study results show that the SFP-BAF model with the angle of 30° achieved the highest efficiency of 88.4%, 86.9%, and 83.9% at a flow rate of 8 L/h, 10 L/h, and 12 L/h, respectively. The benefits of adding aluminium foam to the absorber plate is to increase the absorption of radiant heat energy transmitted from the absorber plate, the storage time of thermal energy, and the thermal efficiency of the collector.

Keywords Solar water heating system; absorber flat-plate; aluminium foam; efficiency.

1. Introduction

The Solar Water Heating System (SWHS) is a water heater equipment that utilizes solar energy for domestic scale needs. The potential generated by this system can reduce the energy demand of the building sector, and peak demand for electricity [1]. Renewable energy sources can be combined with conventional energy sources or energy storage systems [2], as well as smart control element heating minimizes energy cost [3], electricity consumption and pollution [4].

Researchers have worked on a variety of SWHS advances, including changing the shape of the absorber plate, using porous materials, and modifying the transparent cover glass using Fluorine Doped Tin Oxide Nanomaterials [5].

The current development of SWHS is modifying the Flat-Plate Collector (FPC) material. Jalaluddin et al. [6] conducted a study to analyze the thermal efficiency of SWHS using a V-shaped absorber plate. The results showed that the SWHS using a V-shaped absorber plate had an efficiency of 3.6-4.4 % against systems that use standard plates. Further research by Jalaluddin et al. [7], adding phase change material (PCM) to the V-shaped SWHS is increased the average efficiency significantly of 20%, 14% and 13% with flowrates of 0.5; 1 and 1.5 L/min respectively. However, this design has disadvantage due to fluid leakage.

Another development of FPC is by adding porous materials such as asphalt material, aluminium foam and copper foam. Pukdum et al. [8] investigated the performance

of SWHS using asphalt material as an absorber plate. The results showed that the maximum absorber plate temperature was 60 °C, the difference between the water inlet and outlet temperature was 17.2 °C, and the efficiency of SWHS is in the range of 70-79%. Then, Guerroudj and Kahalerras [9] investigated the effect of the design of the shape (rectangular, triangular) and structure of metal foam blocks on collectors. The results show that the square foam block shape is more optimal at high Darcy Number and Reynold Number parameters, resulting in a higher heat transfer rate. In addition, Chen and Huang [10] studied the aluminium foam block parallel under the absorber plate with a certain thickness. This study shows that inserting metal foam blocks at the inner wall of the absorber is an effective method for improving the thermal performance of flat-plate solar water collectors.

Another approach is carried out by Valizade et al. [11] with arrangement a block of copper foam at a certain distance inside the tube on the parabolic collector. The arrangement of the copper foam block increases the thermal efficiency of the collector significantly compared to without the use of the foam block. In addition to developing foam blocks, some researchers use full-filled metal foam in the collector. For steam production, a parabolic trough collector is used since it can produce high temperatures (100-400° C) [12]. In, addition, Baig and Ali [13] used aluminium foam and paraffin blocks in the double pass solar air heater model. The results show that when outside air temperature is maintained between 15-29°C, the four ducts embedded with aluminum foam and paraffin wax without fan obtain maximum efficiency about 97 %.

Saedoddin et al. [14] used full-filled copper foam affixed under the absorber and insulator plates at a 45° angle. The study results showed an increase in absorption heat energy reaching 18.5%, and the Nusselt number increased by 82% compared to the foam material. In addition, the value of the thermal efficiency of the collector also increases with a given flow rate variation. Using metal foam in a filled form was also developed by Anirudh and Dhinarkhan [15]. Simulation analysis through radiation modelling and the Rosseland approach to the inclination angle. The modelling analysis results in the maximum performance occurring at a slope between 15° and 30°, but an increase in the inclination angle more 30° will reduce the efficiency.

In this paper, studies on the use of full-filled aluminium foam at the bottom of the absorber plate have been done by some researchers, but studies of full-filled aluminium foam placed on the top of the absorber plate are still not investigated by researchers as a heat storage material. Based on in this, the full-filled aluminium foam placed on the bottom and the top of the absorber plate was used with the variation on the collector tilt angle and fluid flow rate to evaluate the collector's performance. Therefore, this study aims to analyze the performance of SWHS experimentally by modifying the addition of full-filled aluminium foam material at the bottom and the top of the absorber plate.

2. Experimental Set-up and Description

This research was conducted at the Renewable Energy Laboratory, Mechanical Engineering of Hasanuddin University, Gowa campus (1190 30' 06.1" BT and 050 13' 52.4" LS). As shown in Fig. 1 and its specification shown in Table 1, a solar thermal energy unit is used to investigate the thermal performance of the absorber plate. The equipment is equipped with its lighting unit, a flat-plate collector that absorbs radiation energy and transfers heat to water. Water is circulated through a storage reservoir using a water pump. The reservoir tank has in and out channels for tap water, and heat can be removed if necessary. The water content of the tank can also be heated with integrated heating. The flow rate is controlled via the flow rate potentiometer switch, corresponding to the pump rotation speed. The equipment is also equipped with sensors to detect temperature, lighting, and flow rate.

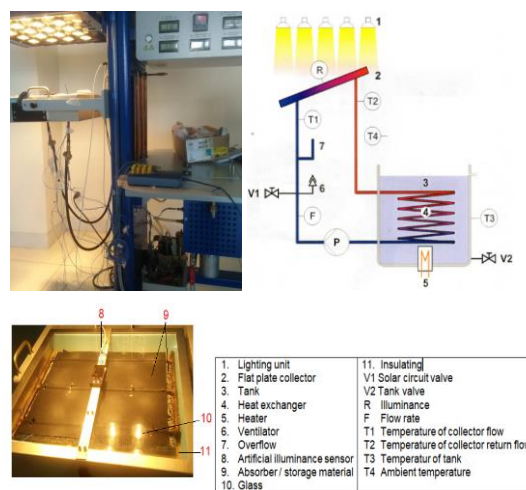


Fig. 1. ET 202 solar thermal energy unit

Table 1. Solar thermal energy unit specifications

Description	Dimension	Unit
<i>ET 202 FPC</i>		
Absorbing surface	320 x 340	mm
Angle adjustment	0-60	deg
Height adjustment	532	mm
<i>Lighting unit</i>		
Halogen lighting units	25 x 50	W
Illuminance	0,5 – 2,5	kW/m ²
<i>Peristaltic Pump</i>		
Variable Flow rate	3 – 20	L/h
<i>Measuring range</i>		
Temperature	0 – 100	°C
Flow rate	0 – 30	L/h
Irradiance	0 – 3	kW/m ²

The test section is a rectangular box with absorber plates and storage materials. In this test, three (3) models of plate absorber such as 1) Standard Flat-Plate (SFP); 2) SFP with Bottom Aluminium Foam (SFP-BAF), and 3) SFP with Top Aluminium Foam (SFP-TAF). The three (3) plate absorber models are presented in Fig. 2. Table 2 shows the

specifications of the absorbent plate model. Experimental testing of each absorber model using a thermal storage unit under the same conditions for 2 hours. Record data of all parameters are recorded automatically at 1-minute intervals. The recorded data are included artificial solar intensity, inlet and outlet fluid temperatures, and flow rate. The recorded measurements and performance analysis while experimenting is made easier thanks to the ET 202 software [16].

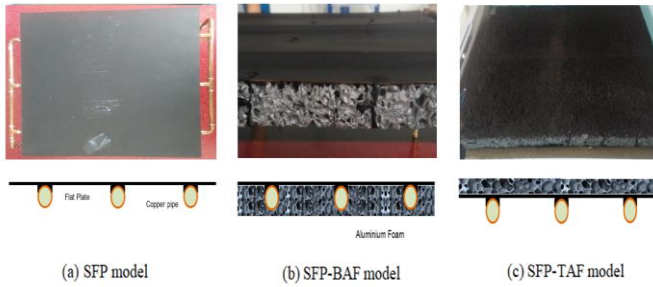


Fig. 2. Collector models

Table 2. Absorber plate specifications

Description FPC	Dimension	Unit
Absorbing plate surface	0,285 x 0,300 x 0,002	m
Pipe diameter	0,008	m
Flow channel cross section	$5,02 \times 10^{-5}$	m ²
Aluminium foam	0,285 x 0,300 x 0,15	m
Flow rate	8, 10, 12	L/h

3. Thermal Performance

In steady state, the performance of a solar collector is described by an energy balance that indicates the distribution of incident solar energy into useful energy gain, thermal losses, and optical losses. The useful energy output of a collector of area A_c is the difference between the absorbed solar radiation and the thermal loss [17]:

$$Q_u = A_c [S - U_L (T_{pm} - T_a)] \tag{1}$$

Q_u , the valuable energy is also calculated based on the temperature measurement data of the inlet and outlet water of the collector specified in equation 2 [18].

$$Q_u = \int Q_u dt = \dot{m} C_p (T_o - T_i) \tag{2}$$

Where m is the mass flow rate (kg/s), C_p is the specific heat (kJ/kg.K) and T_o is the temperature of the fluid leaving the collector (°C), and T_i is the temperature of the fluid entering the collector (°C).

The collector's efficiency is the ratio of the useful gain over some specified time period to the incident solar energy over the same time period [18].

$$\eta = \frac{\int Q_u dt}{A_c \int I_T dt} \tag{3}$$

I_T is the solar intensity (W/m^2), and A_c is the collector surface area (m^2).

4. Results and Discussion

4.1. Solar Intensity

The intensity of solar radiation on the test equipment comes from lighting units measured from an artificial solarimeter. Fig. 5 shows the solar radiation intensity from the three models including SFP, SFP-BAF and SFP-TAF at a tilt of 0° and 10 L/h. Such models tend to be the same solar intensity values about 1.3 – 1.4 kW/m^2 for 1-hour operation.

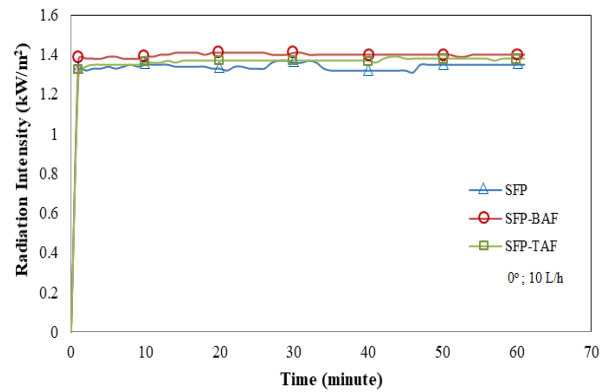


Fig. 5. Radiation intensity based on position

Changes in the angle of inclination on SFP-BAF model is shown in Fig. 6. The angular position of the collector determines the amount of radiation intensity that reaches the glass absorber plate, the reflection of radiation back to the glass and the level of absorptivity of the absorber plate. The maximum radiation intensity is achieved at 0° angle of 1.4 kW/m^2 and the minimum is 30° angle of 1.16 kW/m^2 . This study is in accordance with the results of research conducted by Taheri et al. [19] that an increase in the angle of inclination causes the transmissivity with absorptivity to decrease.

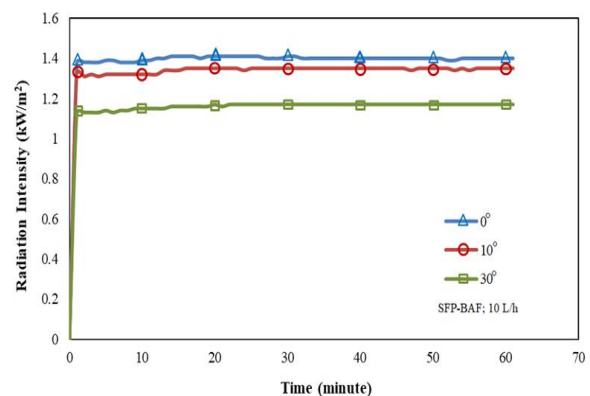


Fig. 6. Radiation intensity based on the tilt angle

Fig.7 shows correlation between flow rate and radiation intensity. It shows that the radiation intensity for all models tends to constant on the flow rate change. Water flow rates of

8 L/h, 10 L/h, and 12 L/h with radiation intensity is approximately 1.3 – 1.4 kW/m².

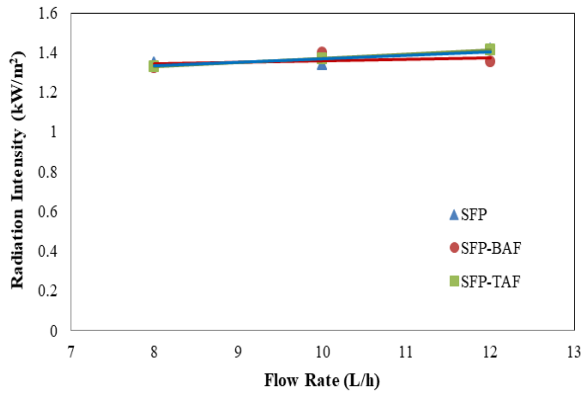


Fig. 7. Radiation intensity based on flow rate

4.2. Inlet and Outlet Water Temperatures

Fig. 8 shows the inlet and outlet water temperatures at an angle of 0° and a flow rate of 10 L/h. Inlet water temperature in all models is between 28-29 °C. The SFP-BAF model has a higher outlet water temperature than other models. The maximum outlet water temperature of the SFP-BAF model is around 46.3 °C for 1 hour. After the heat lighting units are stopped, the temperature of the water inlet and outlet reaches the same temperature at a certain time. The heat stored in the SFP-BAF and SFP-TAF model has a longer storage time than the standard model (SFP). The SFP-TAF and SFP BAF models have a duration time of approximately 30 minutes. The addition of aluminium foam at the bottom of the absorber plate (SFP BAF model) is beneficial in storage heat. This study is in accordance with the results obtained by Prasanth et al. [20] that the fluid temperature increases 2–2.5 times after passing through the heat energy storage material.

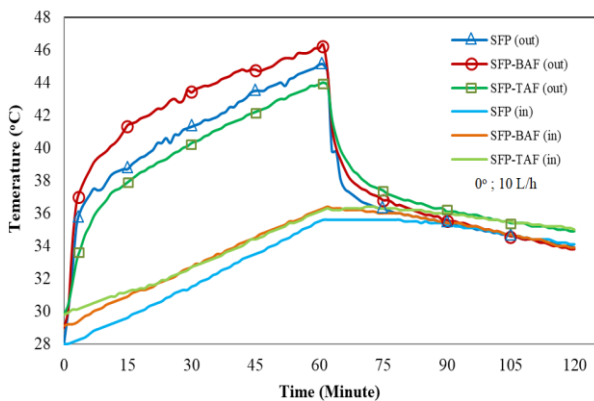


Fig. 8. Water inlet and outlet temperatures based on position models

Fig. 9 shows the inlet and outlet water temperatures at model SFP-BAF at a flow rate of 10 L/h with various inclination angles. The highest outlet water temperature is obtained at an angle of 10° around 47.3 °C, and the lowest is 30° around 45.5 °C. The change in inclination angles from 0 to 30°, causes the heat absorption by the absorber plate to water reduced. After the heat lighting units are stopped, the outlet water temperature at an angle of 10° is still maintained

for 30 minutes. The aluminium foam at the bottom of the absorber plate effectively retains the heat. However, all stored heat is not overall transferred to the circulating fluid. The heat stored in the aluminium foam may be dissipated to the environment. This may be caused by the high dimension difference between the thickness of the aluminium foam and the diameter of the pipe which induces heat to move to the bottom away. The large specific area of the metal foam provides higher heat transfer fluid mixing, heat transfer rates, and thermal performances [10].

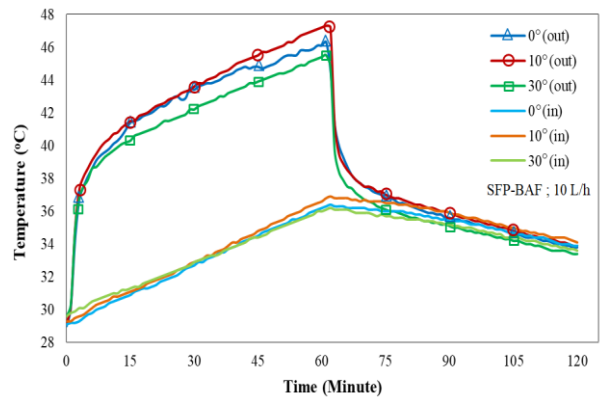


Fig. 9. Water inlet and outlet water temperatures based on tilt angle

Fig. 10 shows the water temperatures of the collector concerning the change in flow rate. All models have the same trend of decreasing the outlet water temperature if the flow rate increases. The SFP-BAF model obtains the maximum outlet temperature value for all flow rates. 8 L/h flow rate has the heat transfer from the absorber plate surface to the fluid is higher than other flow rate. It reaches 47.9 °C. In addition, the addition of aluminium foam also contributes to the effect of transferring heat to the fluid so that the outlet temperature is also high.

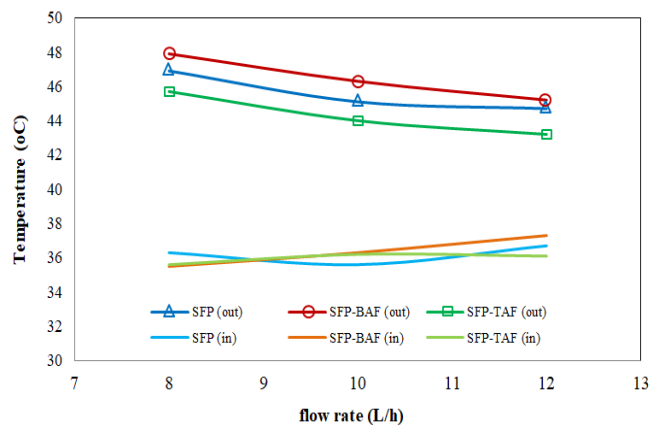


Fig. 10. Inlet and outlet water temperature based on flow rate

4.3. Collector Efficiency

Fig. 11 shows correlation between the thermal efficiency and operation time. In the first 1 hour period, the thermal efficiency reaches the constant after around 20 minutes operation with around 80 percent of efficiency. After 1 hour period, the thermal efficiency of the collector is zero because the intensity radiation is turned off. However, the heat is still

stored in aluminium foam although the intensity radiation is turned off. In addition, the efficiency value tends to decrease along with the increase in the circulating water flow rate. At a flow rate of 10 L/h, the SFP-BAF model is higher efficiency than the other two models. The addition of aluminium foam at the bottom significantly helps absorb heat, store, and retain heat. For increasing the time of heat storage, the specific treatment of aluminium foam needs to modify with reducing the thickness of the aluminium foam.

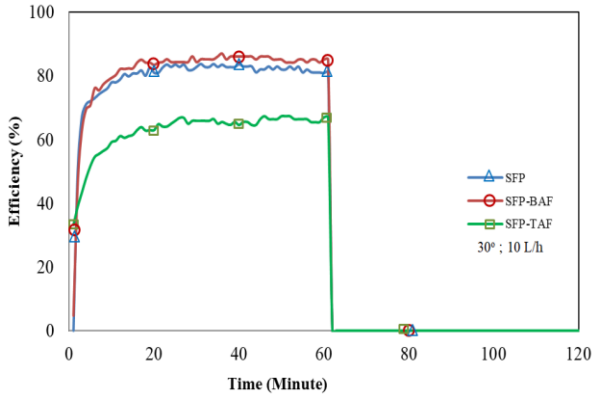


Fig. 11. Collector efficiency based on position models

Fig. 12 shows the efficiency comparison of the slope angle of the SFP-BAF model at a flow rate of 10 L/h. It can be seen that the greater the angle of inclination, the greater the efficiency of the collector. The SFP-BAF model has a maximum thermal efficiency value at an angle of 30° by 86.9% at a flow rate of 10 L/h. The lowest efficiency is obtained at an angle of 0° degrees. The addition of the angle of inclination causes to decrease the radiation intensity consequently reducing the thermal efficiency of the collector. Although collectors' performance with porous materials increases with increasing inclination angle, maximum performance is obtained at intermediate angle, whereas every further increase angle decreases performance [14].

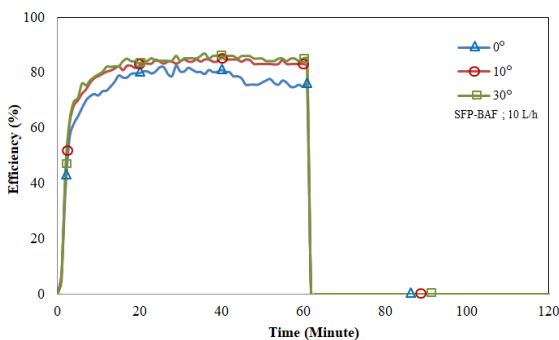


Fig. 12. Collector efficiency SFP-BAF models based on tilt angles

Fig. 13 shows the correlation between the thermal efficiency and flow rate at an angle of 30°. The collector efficiency of the three models tends to decrease with increasing the flow rate. The SFP-BAF model achieved the highest efficiency of 88.4% at a rate of 8 L/h. For flow rates of 10 L/h and 12 L/h, the SFP-BAF model has also the highest efficiency of 86.9% and 83.9%, respectively. The high-efficiency value is due to the low radiation intensity

absorbed by the aluminium foam, but the heat transferred to the fluid is high. The efficiency of the SFP-TAF model tends to constant value of around 70-80%.

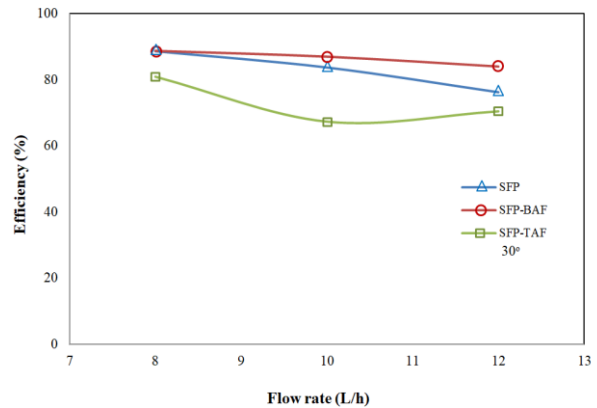


Fig. 13. Comparison collector efficiency based on flow rate

The placement of aluminium foam in the collector can act as an absorber and heat storage. The aluminium foam placed at the bottom of the absorber plate functions more as a heat storage material because it can help increase the water output temperature and retain heat for a particular time. Then, the benefits of adding aluminium foam to the absorber plate is to increase the storage time of thermal energy, and the thermal efficiency of the collector. In contrast, the placement of aluminium foam at the top functions more as a good heat absorber because it can increase the level of heat absorption of the collector.

4.4. Uncertainty analysis

Uncertainty is defined as the imperfection of multiple measuring elements. Uncertainty is caused by a variety of factors, including measurement methods, measuring instruments, operators, and the surrounding environment. The uncertainty analysis is required to assess the correctness of the measure's outcomes. As a result, the data's validity is verified, and a detailed approach for calculating accurate and complete uncertainty is proposed. As shown in Equation (4), the uncertainties that arise as a result of computing (U_R) owing to multiple independent variables.

$$U_R = \left[\left(\frac{\partial R}{\partial x_1} u_1 \right)^2 + \left(\frac{\partial R}{\partial x_2} u_2 \right)^2 + \dots + \left(\frac{\partial R}{\partial x_n} u_n \right)^2 \right]^{1/2} \quad (4)$$

Where the result R is a function in terms of its independent variables as x_1, x_2, \dots, x_n , thus $R = R(x_1, x_2, \dots, x_n)$, u_1, u_2, \dots, u_n are the uncertainties in the independent variables and U_R is the uncertainty of the result.

The temperature of the water inlet, outlet, and flow rate were measured in this investigation using the previously described equipment. Equation (5) is used to determine and quantify the uncertainties of each estimated and measured parameter. The following is how the uncertainty in the temperature of the water inlet, outlet, and flow rate can be calculated [8].

$$Q = f(\dot{m}, C_p, T_i, T_o) \quad (5)$$

$$U_R = \left[\left(\frac{\partial Q}{\partial \dot{m}} u_{\dot{m}} \right)^2 + \left(\frac{\partial Q}{\partial C_p} u_{C_p} \right)^2 + \left(\frac{\partial Q}{\partial T_i} u_{T_i} \right)^2 + \left(\frac{\partial Q}{\partial T_o} u_{T_o} \right)^2 \right]^{1/2} \quad (6)$$

using algebraic manipulation, we were able to acquire

$$\frac{U_Q}{Q} = \left[\left(\frac{U_{\dot{m}}}{\dot{m}} \right)^2 + \left(\frac{U_{C_p}}{C_p} \right)^2 + \left(\frac{U_{T_o}}{T_o - T_i} \right)^2 + \left(\frac{U_{T_i}}{T_o - T_i} \right)^2 \right]^{1/2} \quad (7)$$

Total measurement errors are estimated to be $\pm 0.171\%$ for inlet water temperature and $\pm 0.172\%$ for outlet water temperature. The measured values can be used to compute the mass flow rate. The overall accuracy of the mass flow rate is $\pm 2.4\%$, according to the data.

5. Conclusions

Thermal performances of SWHS by using of full-filled aluminium foam at the bottom and the top of the absorber plate was investigated. The results presented of water outlet and inlet temperature, and thermal efficiency. Based on position, SFP-BAF model have a higher outlet water temperature than the other model around $46.3\text{ }^\circ\text{C}$ at inclination angle 0° and 10 L/h flow rate. Then, based on inclination angle on SFP-BAF, the maximum water outlet temperature have value approximately $47.3\text{ }^\circ\text{C}$ at angle 10° . Lastly, the SFP-BAF model with angle of 30° achieved the highest efficiency of 88.4% , 86.9% , and 83.9% at a flow rate of 8 L/h , 10 L/h , and 12 L/h , respectively.

The benefits of adding aluminium foam to the absorber plate is to increase the absorption of radiant heat energy transmitted from the absorber plate, the storage time of thermal energy, and the thermal efficiency of the collector.

Acknowledgements

This study was supported by the Laboratory-Based Education (LBE) Research Fund 2021, Engineering Faculty of Hasanuddin University.

References

[1] A. Rout, S. S. Sahoo, S. Thomas, and S. M. Varghese, "Development of Customized Formulae for Feasibility and Break-Even Analysis of Domestic Solar Water Heater," *International Journal of Renewable Energy Research*, vol. 7, no. 1, pp. 386–398, 2017.

[2] A. Colak and K. Ahmed, "A Brief Review on Capacity Sizing, Control and Energy Management in Hybrid Renewable Energy Systems," *2021 10th International Conference on Renewable Energy Research and Application (ICRERA)*, pp. 453–458, 2021.

[3] S. Walgama, U. Hasinthara, A. Herath, K. Daranagama and S. Kumarawadu, "An Optimal Electrical Energy Management Scheme for Future Smart Homes," *2020*

IEEE 8th International Conference on Smart Energy Grid Engineering (SEGE), pp. 137–141, 2020.

[4] H. Lill, A. Allik, M. Hovi, K. Loite and A. Annuk, "Integrated Smart Heating System in Historic Buildings," *2019 7th International Conference on Smart Grid (icSmartGrid)*, pp. 92–96, 2019.

[5] V. Msomi and O. Nemraoui, "Improvement of the performance of solar water heater based on nanotechnology," *2017 IEEE 6th International Conference on Renewable Energy Research and Applications (ICRERA)*, pp. 524–527, 2017.

[6] Jalaluddin, A. Effendy, and R. Tarakka, "Experimental Study of an SWH System with V-Shaped Plate," *J. Eng. Technol. Sci.*, vol. 48, no. 2, pp. 207–217, 2016.

[7] Jalaluddin, R. Tarakka, M. Rusman, and A. A. Mochtar, "Performance Investigation of Solar Water Heating System with V-Shaped Absorber Plate Integrated PCM Storage," *International Journal on Engineering Applications (IREA)*, vol. 8(5), 2020.

[8] J. Pukdum, T. Phengpom, and K. Sudasna, "Thermal Performance of Mixed Asphalt Solar Water Heater," *International Journal of Renewable Energy Research*, vol. 9, no. 2, pp. 712–720, 2019.

[9] N. Guerroudj and H. Kahalerras, "Mixed convection in a channel provided with heated porous blocks of various shapes," *Energy Conversion and Management*, vol. 51, pp. 505–517, 2010.

[10] C. C. Chen and P. C. Huang, "Numerical study of heat transfer enhancement for a novel flat-plate solar water collector using metal-foam blocks," *International Journal of Heat and Mass Transfer*, vol. 55, no. 23–24, pp. 6734–6756, 2012.

[11] M. Valizade, M. M. Heyhat, and M. Maerefat, "Experimental study of the thermal behavior of direct absorption parabolic trough collector by applying copper metal foam as volumetric solar absorption," *Renewable Energy*, vol. 145, pp. 261–269, 2020.

[12] M. E. Shayan, G. Najafi, and F. Ghasemzadeh, "Advanced Study of the Parabolic Trough Collector Using Aluminum (III) Oxide," *International Journal of Smart Grid*, vol. 4, pp. 111–116, 2020.

[13] W. Baig and H. M. Ali, "An experimental investigation of performance of a double pass solar air heater with foam aluminum thermal storage medium," *Case Studies in Thermal Engineering*, vol. 14, p. 100440, 2019.

[14] S. Saedodin, S. A. H. Zamzamian, M. E. Nimvari, S. Wongwises, and H. J. Jouybari, "Performance evaluation of a flat-plate solar collector filled with

- porous metal foam: Experimental and numerical analysis,” *Energy Conversion and Management*, vol. 153, pp. 278–287, 2017.
- [15] K. Anirudh and S. Dhinakaran, “Numerical study on performance improvement of a flat-plate solar collector filled with porous foam,” *Renewable Energy*, vol. 147, pp. 1704–1717, 2020.
- [16] K. Boedecker and J. Rohweder, *Experiment Instructions: ET 202 Principles of Solar Thermal Energy*. Germany: Gunt Hamburg, 2015.
- [17] J. A. Duffie (Deceased), W. A. Beckman, and N. Blair, *Solar Engineering of Thermal Processes, Photovoltaics and Wind*, 1st ed. Wiley, 2020.
- [18] N. Roonprasang, P. Namprakai, and N. Pratinthong, “Experimental studies of a new solar water heater system using a solar water pump,” *Energy*, vol. 33, no. 4, pp. 639–646, 2008.
- [19] Y. Taheri, K. Alimardani, and B. M. Ziapour, “Study of thermal effects and optical properties of an innovative absorber in integrated collector storage solar water heater,” *Heat and Mass Transfer*, vol. 51, pp. 1403–1411, 2015.
- [20] N. Prasanth, M. Sharma, R. N. Yadav, and P. Jain, “Designing of latent heat thermal energy storage systems using metal porous structures for storing solar energy,” *Journal of Energy Storage*, vol. 32, p. 101990, 2020.